

NBSIR 88-3790

Electrochemical Evaluation of Solid State pH Sensors for Nuclear Waste Containment

Peter H. Huang
Kenneth G. Kreider

U.S. DEPARTMENT OF COMMERCE
National Bureau of Standards
National Engineering Laboratory
Center for Chemical Engineering
Chemical Process Metrology Division
Gaithersburg, MD 20899

May 1988



75 Years Stimulating America's Progress
1913-1988

Sponsored by:

QC
100
U56
#88-3790
1988
c.2

Regulatory Commission
Research
ton, DC 20555

NATIONAL INSTITUTE OF STANDARDS &
TECHNOLOGY
Research Information Center
Gaithersburg, MD 20899

NBSIR 88-3790

**ELECTROCHEMICAL EVALUATION OF
SOLID STATE pH SENSORS FOR
NUCLEAR WASTE CONTAINMENT**

Peter H. Huang
Kenneth G. Kreider

U.S. DEPARTMENT OF COMMERCE
National Bureau of Standards
National Engineering Laboratory
Center for Chemical Engineering
Chemical Process Metrology Division
Gaithersburg, MD 20899

May 1988

Sponsored by:
Nuclear Regulatory Commission
Office of Research
Washington, DC 20555



U.S. DEPARTMENT OF COMMERCE, C. William Verity, *Secretary*
NATIONAL BUREAU OF STANDARDS, Ernest Ambler, *Director*

20100
- U56
no. 88-3790
1988
C.2

Review of
Electrochemical Evaluation of Solid State pH Sensors
for Nuclear Waste Containment

Contents

	Page
I. Introduction	1
II. Theoretical Models of the Oxide-Liquid Interfaces.....	4
A. The Electrical Double Layer.....	4
B. Modification of Double Layer Model.....	8
III. Electrochemistry of IrO ₂ Films.....	11
A. Formation and Properties of Anodic IrO ₂ Films.....	11
B. Electrochemical Behavior.....	14
IV. pH Testing of Sputtered Iridium Oxide Films (SIROF).....	16
A. Ionic Sensor Principles.....	16
B. pH and its Measurement.....	18
C. Testing to Insure Suitability for Geochemical Metrology.....	21
V. Summary.....	23
References.....	27

I. Introduction

The National Bureau of Standards (NBS) has reviewed technical reports on the high level waste package for nuclear waste storage. The Department of Energy (DOE) waste package test data have been evaluated and compiled by the NBS for the Nuclear Regulatory Commission (NRC) [1]. It is clear from these reports that pH is one of the most important parameters affecting the degradation of the waste packages. Accurate and reliable pH measurement is critical to the satisfactory use of a geochemical code to model the path of reaction between nuclear waste materials, alteration products, and various aqueous solutions. The information obtained for the reaction of nuclear waste materials with aqueous solutions is essential for understanding and predicting the behavior of these materials under repository conditions. The NBS has also reviewed the performance of a number of elevated temperature pH sensing technologies for the NRC [2]. Measurement of pH in a geologic repository requires the use of pH sensor in high pressure and elevated temperature corrosive brines. Recent work of Hodges and Pederson [3] at Pacific Northwest Laboratory (PNL) indicated the chemical composition of brines interacting with a high-level nuclear waste package in salt can affect brine pH produced at high temperatures. However, the hydrogen ion activity of the brine is difficult to measure directly, especially at high temperatures and pressures. The hydrogen ion activity is related to the hydrogen ion concentration through the activity coefficient, the value of which depends on the temperature, the pressure and the composition of the solution of interest. The value of the hydrogen ion activity, therefore the pH, can be determined by the direct measurement of the hydrogen ion concentration in brines, provided the activity coefficient is known.

The instability of the conventional reference electrodes such as calomel or silver/silver chloride electrode is also a problem when measuring pH at temperatures above 100°C. The contamination of the internal reference solution is also a problem if the back pressure becomes greater than the internal pressure. Danielson reported [4] a flowing type of reference electrode, which may be used at high temperatures and pressures.

In a recent report to the Office of Research, Nuclear Regulatory Commission the National Bureau of Standards presented a "Review of Materials for pH Sensing for Nuclear Waste Containment" [2] (NBSIR 85-3237). The review was based on the assumption that higher temperature pH sensors would be needed to evaluate the corrosion potential of containment vessels. The authors described the criteria for pH electrode evaluation, the performance of glass pH electrodes, the developmental program on cubic zirconia electrodes and a summary of research studies of fourteen other exploratory electrode materials. A special emphasis was placed on the most promising of the high temperature electrode materials - IrO₂.

The criteria for selection of a pH electrode for use at temperatures up to 250°C were: linear response from pH 1-14, low ionic and redox interference, long term stability, corrosion resistance, and mechanical robustness. The review of the applicability of the glass electrode concluded that although the recent work at the Pacific Northwest Laboratories (PNL) has indicated useful corrosion resistance in the 150-200°C range, the glass electrode has serious stability problems above 150°C. Other problems with the glass electrode relate to its high impedance, SiO₂ hydrolysis at high pH levels, and lack of mechanical robustness.

Yttria stabilized zirconia pH sensors have been studied by Niedrach [5], at General Electric, Tsuruta and Macdonald [6] at SRI, and Danielson at PNL. Generally these ZrO₂(Y) sensors are linear between pH 3-9 and at temperatures above 150°C to 300°C, and exhibit few interference problems if any. The inconvenience of poor room temperature performance, however, complicates the calibration and flexibility of the sensor. The results of research on palladium hydride and numerous metal oxide films for use as pH electrodes are also discussed in the NBS/NRC review including Sb₂O₃, MoO₂, MnO₂, TiO₂, Ta₂O₅, ZrO₂, OsO₂, PdO, PtO₂, RhO₂, RuO₂, and IrO₂. Of these, the IrO₂ emerges as the most promising primarily because of its wide range of stability (both pH and T), its low impedance in thin films and its consistent Nernstian-linear response.

The remainder of the review by Dietz and Kreider outlines the research

findings in IrO₂ pH sensor studies, the key questions to be answered and a suggested approach for developing the reactively sputtered IrO₂ film as a high temperature, harsh environment sensor.

In order to develop the pH electrode for use at high temperatures and pressures and to understand the interaction between the electrode and the solution, quantitative information about the electrochemical behavior at the oxide-solution interface is essential. One of the fundamental factors determining all electrochemical phenomena occurring at the solid-liquid interfaces is the electric charge and potential distribution in these regions. The simplest model reflecting the real electrical structure of the interface region is the electrical double layer (e.d.l) model. An electrical double layer occurs at all interfaces and its structure depends on the properties of the contacting phases. Knowledge of the structure of the electrical double layer and the charge and potential distribution in the layer is very important because it will greatly influence or determine such pH electrode phenomena as hydrogen ion sensitivity and selectivity, open circuit potentials, electrode stability and others.

Therefore, improved understanding of the electrochemical behavior at the IrO₂-solution interface is needed to optimize the performance of IrO₂ electrodes for pH sensing at high temperatures and pressures.

Several workers have attempted to quantitatively describe the charge and potential distribution at the oxide-liquid interface using various theoretical models. These models are described in Section II.

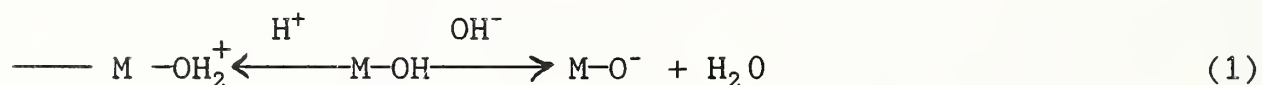
Hydrous oxides are of major interest in the areas of technology such as aqueous battery systems, colloid chemistry, electrochromic display systems and pH sensing. Hydrous iridium oxide films are of special interest since iridium oxide has been shown to have good chemical stability in aqueous solutions at temperatures up to 200°C [7]. In Section III of this report, the electrochemical preparation, redox behavior, and some important properties of hydrous iridium oxide films are described.

Section IV describes pH testing of sputtered iridium oxide films (SIROF). The general principles of ionic sensing are briefly described, followed by a discussion of pH measurement methods. The scope of testing for geochemical metrology is then described for geochemical measurements.

A summary of this report is presented in Section V.

II. Theoretical Models of the Oxide-Liquid Interfaces

This section reviews theoretical models used to describe the e.d.l for colloidal metal oxide systems. The surface charge and potential of an insoluble metal oxide is determined in large part by the pH of the solution in which it is immersed. For such systems the OH⁻ and H⁺ ions are potential-determining ions as a result of the following reactions



where M represents metal. The presence of hydroxyl groups on metal oxide surfaces has been amply demonstrated by infrared spectroscopy. Theoretical models useful for describing the electrochemical behavior of a colloidal system may not be strictly applicable to iridium oxide, which has a metal-like conductivity. Based on the more recent studies of metal-liquid and semiconductor-liquid interfaces, however, useful information may be obtained to characterize electrochemical properties of iridium oxide-liquid systems within the framework of the theoretical models described in this section.

A. The Electrical Double Layer

In this section, no attempt is made to cover all studies of the oxide-liquid interface. Recent work is reviewed to obtain the important facts that are relevant to the nature of the interface. A considerable amount of work in this area has also been reviewed by Lyklema [8,9], Ahmed [10], Hunter [11], and Parsons [12].

The double layer model is the classical approach to describe the electrical structure of the solid-liquid interface and is usually referred as

the Gouy-Chapman-Stern-Grahame (GCSG) model. In this model, the electrical double layer consists of two regions: an outer diffuse region and an inner Helmholtz region. In the outer diffuse region, the ions undergo thermal Brownian motion and are distributed according to the Boltzmann statistics. The inner Helmholtz region has two planes. The inner Helmholtz plane (IHP) is the plane of the centers of adsorbed ions near the solid surface. The outer Helmholtz plane (OHP) is the plane of the centers of hydrated ions near the diffuse region.

The mean electrical potential at any point in the diffuse layer satisfies the well-known Poisson-Boltzmann equation

$$\nabla^2 \phi = -(e/\epsilon\epsilon_0) \sum z_i n_i \exp(-z_i e\phi/kT) \quad (2)$$

where ϕ is the mean potential, n_i is the number of ions of type i per unit volume in the liquid phase, z_i is their valency with sign, e is the unit of electric charge, ϵ is the dielectric constant of the medium, ϵ_0 is the permittivity of free space ($8.854 \times 10^{-12} \text{ Fm}^{-1}$), k is the Boltzmann's constant and T is the absolute temperature. For a flat interface, Eq. (2) is solved with the boundary conditions $\phi=\phi_d$ at $x=0$, where ϕ_d and x are the potential and the coordinate, respectively, at the OHP and $d\phi/dx=0$ at $x=\infty$. The solution is given by

$$\phi = (2kT/ze) \ln [1 + \gamma \exp(-\alpha x)] / [1 - \gamma \exp(-\alpha x)] \quad (3)$$

where $\gamma = \exp[(ze\phi_d/kT)-1] / \exp[(ze\phi_d/kT)+1]$, and $\alpha = 2z^2 e^2 n_i / \epsilon\epsilon_0 kT)^{1/2} = 3.29 \times 10^9 z(c)^{1/2} \text{ m}^{-1}$ at 298K, and c is the bulk electrolyte concentration in mol dm^{-3} .

The diffuse layer charge density, σ_d , contained in a cylinder of unit cross-sectional area extending from $x=0$ to $x=\infty$ is given by

$$\sigma_d = -(8n_i \epsilon\epsilon_0 kT)^{1/2} \sinh(ze\phi_d/2kT)$$

$$= -11.74 (c)^{1/2} \sinh (19.46 z\phi_d) \mu\text{C cm}^{-2} \quad (4)$$

at 298 K, where ϕ_d is in volts.

The surface charge density of adsorbed ions at IHP is given by the Stern adsorption isotherm

$$\sigma_\beta = \frac{z_+ e N_a}{1 + (A_o/n_+ M) \exp[(z_+ e \phi_\beta + \Phi_+)/kT]} + \frac{z_- e N_a}{1 + (A_o/n_- M) \exp[(z_- e \phi_\beta + \Phi_-)/kT]} \quad (5)$$

where z_\pm is the valency of cations or anions with sign, N_a is the number of available adsorption sites, A_o is Avogadro's number, n_\pm is the bulk concentration of the ionic species in ions/cm³, and M is the relative molecular mass of the solvent. Φ_\pm are specific adsorption potentials that account for non-Coulombic interactions, such as changes in the state of solvation of the adsorbed ions, van der Waals interactions, or hydrogen bonding between the adsorbate and the surface. When these non-Coulombic interactions contribute significantly to the free energy of adsorption of ions, the adsorption is said to be specific [13]. A specifically adsorbed ion can therefore adsorb against electrostatic repulsion such that σ_β in Eq. (5) is greater than σ_o , the surface charge density at the solid surface. This leads to a reversal of the signs of the diffuse layer charge and potential. This possibility is of great importance for the case of adsorption of H⁺ or OH⁻ ions which are chemically bound.

Because of electroneutrality, the charge densities at the surface, the IHP and the OHP are related by

$$\sigma_o + \sigma_\beta + \sigma_d = 0 \quad (6)$$

If the potential drop between each plane is assumed to be linear, the integral capacity per unit area, C_1 , of the zone between the surface and the IHP is given by

$$C_1 = \sigma_o / (\phi_o - \phi_\beta) = \epsilon_1 \epsilon_o / \beta \quad (7)$$

where ϵ_1 and β are the dielectric constant and separation between the surface and the IHP, respectively. The integral capacity per unit area between the IHP and the OHP, C_2 , is given by

$$C_2 = -\sigma_d / (\phi_\beta - \phi_d) = \epsilon_2 \epsilon_o / d \quad (8)$$

where ϵ_2 and d are the dielectric constant and separation between the IHP and the OHP, respectively. Hence the five equations (4) to (8) relate to six variables σ_o , σ_β , ϕ_o , ϕ_β , and ϕ_d of the GCSG model of the electrical double layer. Thus, if one of these six variables is known then the others may be computed provided that the values for the parameters N_a , Φ_\pm , C_1 , and C_2 are also known.

The total double layer differential capacity, $d\sigma_o/d\phi_o$, can be obtained by combining Eqs. (7) and (8) to give ϕ_o ,

$$\phi_o = \sigma_o / C_1 - \sigma_d / C_2 + \phi_d \quad (9)$$

and then differentiating with respect to σ_o

$$d\phi_o/d\sigma_o = (1/C_1) - (1/C_2)(d\sigma_d/d\sigma_o) + (d\phi_d/d\sigma_d)(d\sigma_d/d\sigma_o) \quad (10)$$

where C_1 and C_2 are assumed to be independent of σ_o . The diffuse layer capacitance, $C_d = -(d\sigma_d/d\phi_d)$, is obtained from Eq. (4) and $(d\sigma_d/d\sigma_o)$ may be expressed in terms of σ_β by using Eq. (6). Therefore the total differential capacitance, C , is given by

$$C^{-1} = d\phi_o/d\sigma_o = (1/C_1) + (1 + d\sigma_\beta/d\sigma_o)(1/C_2 + 1/C_d) \quad (11)$$

Calculated capacitance may then be compared with the experimental differential capacitance.

In the simple GCSG model described above, the surface charge densities are assumed to be uniformly distributed in each plane. The effect of discreteness of charge has been introduced by Levine, Bell and co-workers [14,15] to account for various phenomena, e.g. adsorption at the mercury-water interface.

Blok and de Bruyn [16] were the first to describe a GCSG-based model for an oxide-liquid interface. They assumed ideal Nernstian behavior for the surface potential and compared calculated σ_o - ϕ_o curves for different values of the parameters with their experimental σ_o -pH curves for ZnO electrolyte solutions. Using the following parameter values: $C_1=C_2=100 \mu\text{F cm}^{-2}$ for Eqs. (7) and (8); $\Phi_+ = -2kT$, $\Phi_- = -4kT$, and $N_a = 10^{15} \text{ cm}^{-2}$ for Eq. (5), good agreement between the theoretical and experimental results was obtained.

Later, Levine and Smith extended this basic model to allow for non-Nernstian behavior of the surface potential. They obtained calculated σ_o -pH, C-pH, and ϕ_d -pH curves in reasonable agreement with published experimental data. The double layer properties SnO_2 , SiO_2 , and quartz were investigated by Ahmed et al. [17], Tadros et al. [18], and Li et al. [19] through the use of σ -pH curves. The curves were convex for these oxides. In fact, for all oxides studied so far [20-26] including TiO_2 , $\gamma\text{-Al}_2\text{O}_3$, $\alpha\text{-Fe}_2\text{O}_3$, and MnO_2 , the slope $\partial\sigma_o/\partial\text{pH}$ increases with pH without any indication of reaching a plateau. This phenomenon has been explained by assuming that oxide surfaces are somewhat penetrable for H^+ , OH^- , and counterions [27]. The consequence is that σ_o is not a surface charge but rather a volume charge. Healy et al. [22] have noted that oxides generally exhibit very high charge density values attributed by the charge-determining H^+ or OH^- adsorbed ions.

The GCSG model in general can account for observed interfacial properties provided certain values are assigned for various parameters (e.g., specific adsorption potential, inner layer surface charge density). However, it has been pointed out that it is not at all certain that the parameter values assigned are reasonable [22].

B. Modification of Double Layer Model

In order to explain the phenomena associated with the very high surface charge densities observed at oxide-solution interfaces as mentioned before, various nonclassical models have been proposed. These models include the porous double layer model [27-29], the gel layer [30-32], the transition layer model [33,34], and the site-binding model [35-37].

(a) Porous double layer model [27-29]--This model assumes that the oxide surface is porous to charge-determining ions and counterions. This approach accounts at least qualitatively for the general trends observed in interfacial properties. The surface charge is substantially higher in solutions of certain ions that can penetrate the solid than in solutions of other ions. For example, in 10^{-1} M LiCl at pH 10, on hematite, σ_0 is almost twice as high as in 10^{-1} M KCl, apparently because Li^+ can penetrate into the solid, thereby occupying Fe^{+3} -sites. Penetration distances of less than 1 nm are usually needed to account for the observed high charges [27]. The theory indicates that high valence charges require much counterion compensation, therefore the charge remaining in the diffuse double layer part is comparatively small.

(b) Gel layer model [30-32]--This model assumes that there is a homogeneous gel-like layer of definite thickness (2-5 nm) at the interface containing metal hydroxy groups $\text{M}(\text{OH})_n$ into which various ions can adsorb. This model accounts for the high surface charge in terms of ion penetration into subsurface regions of the oxide.

(c) Transition layer model [33,34]--This model combines the basic ideas of porous and hydrolyzed gel-like layer theories for the oxide-solution interface. The essential feature of this model is the existence of a transition layer of atomic dimensions in which an equilibrium between oxide and aqueous ionic species is established.

(d) Site-binding model [35-37]--This model assumes that the adsorbed electrolyte cations and anions are distributed in two ways: first, as interfacial ion pairs formed with oppositely charged surface groups, and second, in a diffuse layer to balance the remaining unneutralized surface

charges. Potential-determining ions and counterions are considered to react or bind with the acid-base sites on the oxide surface. This model is generally adequate for accounting for the shapes of σ_0 -pH curves and specific ion effects [38]. In this model the high surface charge is rationalized in terms of ion-pair formation between surface ionized groups and counterions. Yates et al. [36] assumed that a porous hydrated oxide surface layer at the interface is penetrated by supporting electrolyte ions.

The site-binding model was recently applied to study the temperature coefficient of the metal oxide-liquid interfacial potential as a function of pH for ion-sensitive field-effect transistors (ISFET's) [39]. At electrochemical equilibrium, the electrochemical potentials for a metal oxide-liquid system are given by

$$\begin{aligned} & \mu_{\text{MOH}_2}^{\circ+} + kT \ln \nu_{\text{MOH}_2}^+ + q\phi \\ & = \mu_{\text{MOH}}^{\circ} + \mu_{\text{H}^+}^{\circ} + kT \ln \nu_{\text{MOH}} + kT \ln a_{\text{H}^+} \text{ and} \end{aligned} \quad (12)$$

$$\mu_{\text{MOH}}^{\circ} + kT \ln \nu_{\text{MOH}} + q\phi = \mu_{\text{MO}^-}^{\circ} + \mu_{\text{H}^+}^{\circ} + kT \ln \nu_{\text{MO}^-} + kT \ln a_{\text{H}^+} \quad (13)$$

where M represents metal, μ_x° is the standard chemical potential for the x's species, ν_x is the activity of the x's species at the surface, k is the Boltzmann constant, q is the electronic charge, and ϕ is the potential difference developed at the interface and is given by

$$\phi = q(\nu_{\text{MOH}_2}^+ - \nu_{\text{MO}^-})/C_H \quad (14)$$

where C_H is the capacitance per unit area across the electrical double layer. Eq. (14) is valid if we neglect space charges in the diffuse layer.

It can be shown that the surface potential, the number of active surface sites, the pH, and the temperature are related by the following equation

$$a_{\text{H}^+} = \{K_1 \eta + [K_1^2 \eta^2 + 4(1-\eta^2)K_1 K_2]^{1/2}\} \exp(q\phi/KT)/2(1-\eta) \quad (15)$$

where a_{H^+} is the activity of H^+ , K_1 and K_2 are the dissociation constants given by

$$K_1 = \exp[\mu_{\text{MOH}_2}^{\circ+} - \mu_{\text{MOH}}^{\circ} - \mu_{\text{H}^+}^{\circ}]/kT \quad (16)$$

$$K_2 = \exp[\mu_{\text{MOH}}^{\circ} - \mu_{\text{MO}^-}^{\circ} - \mu_{\text{H}^+}^{\circ}]/kT \quad (17)$$

and η is given by

$$\eta = \phi C_{\text{H}}/qN_s \quad (18)$$

in which N_s is the density of available active sites per unit area at the metal oxide surface. Eq. (15) was used to determine the temperature characteristics of silicon nitride pH-ISFETs for various pH values. Good agreement was obtained between theory and experiment [39].

The site-binding model has been extended to a two-site theory [40] for explaining the features of the potential-pH response of both silicon nitride and borosilicate glass ISFETs. The theory was used to interpret the behavior of chemically treated gate materials for SiO_2 and Ta_2O_5 ISFETs as pH sensing devices [41].

III. Electrochemistry of IrO_2 Films

A. Formation and Properties of Anodic IrO_2 Films

Burke and Lyons [42] have recently surveyed both the theoretical and the experimental work that have been done on hydrous oxide films on several noble metals including platinum, palladium, gold, iridium, rhodium, and ruthenium. This section is concerned only with the electrochemical formation and redox properties of the hydrous IrO_2 films.

One of the most convenient techniques used to generate hydrous oxides in a form suitable for studying their redox behavior is that of potential cycling [43-45]. In this case the potential of the parent metal electrode, which may be noble or non-noble, is cycled repetitively between suitable limits in an aqueous solution of appropriate pH. A sinusoidal,

square, or triangular potential wave form may be used for hydrous oxide film growth. The triangular wave is most commonly implemented because cyclic voltammetry can then be used to monitor the growth and redox behavior of the iridium oxide film.

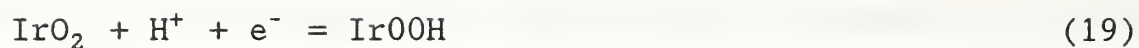
The mechanism of hydrous oxide growth on repetitive cycling is now reasonably well understood, at least at a qualitative level. For most metals, but especially gold, platinum, iridium, and rhodium, extension of oxide growth beyond the monolayer level under conventional galvanostatic or potentiostatic conditions is usually quite slow. Under potential cycling conditions the anodic limit plays quite a crucial role for anodic oxide film formation. The early work on the initial stages of anodic oxide formation on Ir was described by Belanger et al. [46]. Thick oxide films were readily generated on cycling the potential over the normal potential range of 0-1.5 V. It is now generally accepted that cycling the potential of Ir in a wide variety of electrolytes between certain limits induces irreversible formation of a battery-type, porous, hydrous oxide layer [37] whose thickness increases with increasing number of cycles.

On the other hand, the monolayer oxide growth on Ir has been investigated by several researchers. Rand and Woods (44) used a solution of $5 \text{ mol} \cdot \text{dm}^{-3}$ H_2SO_4 , in which the hydrous material is soluble, and observed hydrogen peaks on the anodic sweep at 0.09 and 0.25 V, with oxygen adsorption commencing above 0.4 V. Two very broad peaks were observed in the oxygen adsorption region at 0.7 and 1.0 V, respectively. Similar behavior was also reported by Mozota and Conway [47]. They assumed that a monolayer of OH species was formed in the region of 1.1-1.2 V, conversion to an IrO monolayer being completed at 1.4 V.

The conditions required to produce a thick hydrous oxide layer on iridium under potential cycling conditions were investigated by Buckley et al. [48] and Conway and Mozota [49]. The optimum upper and lower limits in acidic media were found to be 1.60 and 0.01 V, respectively. Oxide growth on cycling was observed with the upper limit just above 1.4 V. Significant penetration of oxygen into the second, or even the third, layer of metal atoms of the bulk

lattice is probable. Increasing the upper limits above 1.6 V causes dissolution of oxide species at the interface. Critical values for both upper and lower limits required for oxide growth on cycling are influenced by a range of kinetically and thermodynamically important factors, e.g., sweep rate, solution composition, temperature, degree of oxygen penetration, and oxide stability. Among other factors which affect the hydrous oxide growth reaction are sulfuric acid concentration, pH, the presence of chloride ions and temperature [43,49-51]. The presence of chloride ion in solution is assumed to inhibit the formation of an anodic oxide film on a clean iridium surface [43]. This effect can be explained in terms of specific adsorption of chloride ions onto the iridium surface in aqueous solution. However, the oxide layer region of the cyclic voltammogram of iridium was unaffected by the addition of chloride [43]. The rate of growth of iridium oxide films depends on the type of and concentration of supporting electrolyte. It decreases in the order $0.5\text{M H}_2\text{SO}_4 > 1\text{M HClO}_4 \gg 0.5\text{M Na}_2\text{CO}_3 \gg 0.5\text{M NaOH}$ [49]. This order follows qualitatively the order of decreasing specific adsorption of the anions and presumably arises from the effects of these ions on the continuing monolayer formation and reduction that takes place on the iridium substrate beneath the growing hydrous oxide film. Cruz et al. has discussed the effect of temperature on the potentiodynamic behavior of iridium in $0.5\text{ M H}_2\text{SO}_4$. It may be assumed that increasing the temperature modifies the structure and composition (degree of hydration) of the highly hydrated oxide layer formed under continuous potential cycling [51]. This modification can then change the physical and electrochemical characteristics of the surface oxide layers on iridium.

Rand and Woods [44] postulated that cycling an iridium electrode in acid resulted in irreversible oxide formation at the metal surface. However, they assumed the material to be a porous form of the anhydrous oxide, IrO_2 , attributing the density value of 11.68 g/cm^3 of the latter to the surface layer. Buckley and Burke [43,48] claimed that the layer formed was a hydrated oxide or oxyhydroxide, such as $\text{IrO}_2 \cdot 2\text{H}_2\text{O}$. They used a redox transition between the Ir(III) and Ir(IV) states in the surface layer to explain the main charge storage reaction:



Mitchell et al. [52] showed that the film formed on cycling in acid was quite rough and not very adherent based on preliminary electron microscopy work. The grain size was quite small (< 50 nm). It was suggested that the film was amorphous having a hexagonal structure. Gottesfeld and Srinivasan [53] showed that potential cycling resulted in the formation of relatively thick film (250 nm after 15 hours of cycling), which they suggested was a hydrated hydroxide. By combining coulometric with optical data, McIntyre et al. [54] found that the apparent density of the hydrous material was 2.0 g cm^{-3} , i.e., one-sixth of that of an hydrous IrO_2 . They showed, using electron microscopy, that the film was porous, with microvoids on the order of 2.5 nm diameter.

Hackwood et al. [55] carried out a combined thermal and gas evolution analysis of sputtered iridium oxide films and suggested these were probably not as dispersed or hydrated as films produced by cycling. Some water was lost in heating in vacuum at 120°C and it was assumed that an amorphous to crystalline transition occurred at 300°C .

Augustynski et al. [56] studied films produced by potential cycling and it was found that the initial layer was not IrO_2 but the hydrated hydroxide. The water was assumed to be chemisorbed on the surface beneath the $\text{Ir}(\text{OH})_4$ species.

B. Electrochemical Behavior

The electrochemical behavior of acid-grown hydrous iridium oxide films are affected by: (i) the acidity of the hydrated material and the variation of this property with change in the iridium oxidation state [57]; and (ii) the difference in electrical conductivity between the reduced and oxidized forms of the surface film [58,59]. According to Burke et al. [60], both properties are strongly dependent on the dispersed hydrated nature of the iridium oxide layer. Both oxidized and reduced forms were assumed to be polymeric network structures. There has been considerable controversy in the literature as to

whether cations [61-63] or anions [64-67] act as charge balancing ions for maintaining electroneutrality in the film in the course of electron insertion or withdrawal reactions.

The ac impedance measurements by Glarum and Marshall [58], and faradaic experiments by Gottesfeld [68], have shown that the hydrous film in the reduced state, Ir(III), has a low electronic conductivity while in the oxidized state, Ir(IV), it is highly conductive. Gottesfeld has interpreted this behavior in terms of conventional band theory. However, Burke and Whelan [60] have proposed a chemical approach involving electron hopping between neighboring Ir centers for interpretation of this behavior. The high conductivity of the oxidized state was attributed to the presence of Ir(VI) sites that behave as acceptor states in the predominantly Ir(IV) film. The direct evidence for these Ir(VI) sites was obtained by ESCA investigation of the oxidized state [56].

In sulfuric acid media [69] a shoulder is usually observed at 0.6 V on the cathodic side of the main anodic peak. According to Burke and Whelan [57] it is probably an Ir (III/IV) transition in species containing anions other than OH^- within the hydrated material. Conway and Mozota [49] attributed the large currents above the main anodic peak mainly to charging of the rather extensive oxide-solution interface. However, Burke and Whelan [57] assumed that the dispersed, hydrated oxide material scarcely constituted a distinct phase, and postulated that the currents in this region were due to changes in stoichiometry in a mixed valence state, Ir(IV)/Ir(VI). A peak showing a shift of $3/2$ (2.303 RT/F) V/pH can be observed [60] above the main anodic peak on transferring an acid grown film to solutions of higher pH. Such a peak was also observed [70] following transfer of a base-grown film to acid.

Although hydrous iridium oxide deposits grown in acid show little change in redox activity on transfer to base, it was demonstrated by Buckley et al. [48] that the film could not be grown on cycling a clean iridium electrode in such a medium ($1.0 \text{ mol.dm}^{-3} \text{ NaOH}$, 0.01 to 1.50 V, 30 VS^{-1}). In a detailed investigation, it was confirmed [70] that hydrous oxide formation was possible in dilute, though not in strong, base. It was also observed that after

subjecting the electrode in base to preliminary cathodic pretreatment, which probably involved removal of any residual oxide film, no growth was observed. This result was explained by assuming that local pH changes within the pores of a superficial oxide layer play a crucial role in the conversion of anhydrous to hydrous oxide.

The base-grown films were found to dissolve readily in $1.0 \text{ mol.dm}^{-3} \text{H}_2\text{SO}_4$ or NaOH and this was attributed to their more amorphous character. On the other hand, the acid-grown films were found to be more crystalline having larger grain sizes and this was used to explain their greater stability in acidic media [70].

Yuen and Lauks [71] showed significantly different cyclic voltammograms for anodically grown and sputtering deposited iridium oxide films. An anodic iridium oxide film had a pH dependent voltammogram. The results of the voltammogram and the derived density-of-states at the Fermi level for the case of a sputtered iridium oxide film (SIROF), however, are independent of pH. It was suggested that the SIROF had a more disordered structure in acidic and alkaline electrolytes.

Reactively sputtered iridium oxide films were shown to have good chemical stability against corrosive environments even at high pressures and temperatures. An extensive series of open circuit potential measurements on d.c. reactively sputtered iridium oxide films was performed for the pH range of 3 to 10. The testing showed promising results for sputtered iridium oxide films as pH probes [7]. An IrO_2 electrode was used by Fog and Buck [72] as a pH sensor and showed near-Nernstian behavior in the pH range of 2 to 12. Unfortunately, IrO_2 as a pH sensor material is subject to instability, ionic interference, and hysteresis effects [7,72]. The instability was attributed to a change in the physical and electrochemical properties of the oxide with time [73]. Kreider et al. also observed a shift of open circuit potential with air baking and autoclave heating at high temperature and pressure [4,74].

IV. pH Testing of Sputtered Iridium Oxide Films (SIROF)

A. Ionic Sensor Principles

Described here is a conventional electrochemical electrode for sensing of ions. The other new chemically sensitive electronic devices can be found in reference [75]. A solid membrane separating two liquids of different ionic content can develop an electrical potential difference across it. This phenomena can be expressed by the Nernst equation

$$E = \frac{RT}{nF} \ln \left(\frac{a_1}{a_2} \right) \quad (20)$$

where E = voltage

R = universal gas constant = 8.32 J/mol.K

T = temperature, K

F = Faraday constant = 9.65×10^4 C/mol

n = ionic change

a_1 = activity of ion to be measured in solution on one side of membrane

a_2 = activity of same ion in solution of other side of membrane

The ionic activity is related to ionic concentration, c, by

$$a = \gamma c \quad (21)$$

where γ is the activity coefficient and has a value of one for highly dilute electrolytes. In Eq. (20), if a_2 of the reference solution is known, then a_1 of the measurand can be determined provided that no other ions are present which would interfere with the measurand.

For ionic sensors using a solid membrane, a basic problem is making electrical contact with the solutions. If metal electrodes were used for this purpose, then additional voltages would be generated in the electrical circuit

due to the chemical reactions at the electrode surfaces. In general, a stable and reproducible ionic sensor requires half cells coupled to the electrolytes by salt bridges or buffer solutions. A half cell consists of an electrode immersed in an electrolyte with which it is in electrochemical equilibrium. Only half cells with electrochemically reversible cell reactions give reproducible results and are useful. The calomel cell (mercury in contact with mercurous chloride/potassium chloride paste) and the silver/silver chloride cell are the most common reference cells.

The output voltage at 25°C is given by

$$E = E^{\circ} + \frac{0.059}{n} \log (\gamma c) \text{ volts} \quad (22)$$

where E° is a constant for the particular configuration of electrode materials and n is the number of ionic charge. A high-input impedance is required so that the voltage may be measured at near zero current. Traditionally this type of ionic measurement is referred to as open circuit potentiometry.

B. pH and Its Measurement

Hydrogen ion concentration is usually defined by the logarithmic measure of pH, i.e.,

$$\text{pH} = \log (1/C_{\text{H}^+}) \quad (23)$$

At 25°C the concentration of H^+ and OH^- ions in pure water is 10^{-7} mol dm^{-3} each. pH values are temperature dependent because the extent of H_2O

dissociation increases with temperature. At 100°C pure water has a C_{H^+} of 10^{-6} mol dm^{-3} , i.e., the pH is 6, but the water is neutral. The product (C_{H^+}) (C_{OH^-}) remains constant when the concentration of either ionic species in an aqueous solution is increased by addition of a solute.

It has been found that the conventional glass pH electrode has a good selectivity for H^+ . Its construction, operating principle, and the composition of the glass are discussed in detail in references 73 and 74. Its operation involves ion transport through a thin glass membrane, made from a glass containing appropriately chosen ionic constituents. The overall mechanism of pH sensing, however, is not simple. The glasses are formulated for optimum behavior under specific conditions of use. Soda glasses containing sodium ions are generally inaccurate above pH 9; lithia extends the range to about 13. Glasses incorporating tantalum, niobium, or rare earth oxides having lower electrical resistance can be used to make thicker glass membranes for electrodes.

General purpose glasses can measure pH from 0 to about 12 at temperatures from 0 to near 100°C (and sometimes beyond). Their electrical resistances at 25°C are in the several hundred megaohm range, the exact value depending on glass composition and membrane thickness. Resistance of the glass varies exponentially with temperature. A glass whose resistance is 100 megaohms at 25°C may be around 1000 megaohms at 0°C and 1 megaohm at 80°C. General purpose glasses show an interference response to sodium ions above approximately pH 10. Glasses formulated for use at higher pH show a greatly reduced response to sodium and other alkali metal ions but also have a higher

electrical resistance, five or more times that of general purpose glass.

The measurement of hydrogen ion activity uses a galvanic cell constructed by combining the glass electrode with a reference electrode, usually the saturated calomel electrode or silver/silver chloride electrode.



The emf of this cell is given by

$$E = E(\text{Cal}) - E'(\text{glass}) + E_L + (2.303 RT/F)\text{pH} \quad (24)$$

where the liquid junction potential, E_L , at the analyte and saturated KCl interface has been included. If one uses the formal definition of pH of Eq. (23), then the pH value of the analyte cannot be deduced from Eq. (24) unless the liquid junction potential is known. Therefore, the formal definition of pH has been replaced by form of Eq. (24). Consider the measurement of the cell emf for a buffer solution of known pH. If the pH value is pH_s and the emf value E_s , then Eq. (24) can be written as

$$E_s = E(\text{Cal}) - E'(\text{glass}) + E_L + (2.303 RT/F)\text{pH}_s \quad (25)$$

For an analyte solution of unknown pH, if the pH value is pH_u and the emf value E_u , then Eq. (25) becomes

$$E_u = E(\text{Cal}) - E'(\text{glass}) + E_L + (2.303 RT/F)\text{pH}_u \quad (26)$$

Assume that the liquid junction potential does not change in changing the standard buffer solution for the unknown pH analyte, then from Eqs. (25) and (26), one obtains

$$\text{pH}_u = \text{pH}_s + (E_u - E_s)/(2.303 RT/F) \quad (27)$$

Here we have noticed that the definition of pH is based on carefully defined buffer solutions. The National Bureau of Standards (NBS) has proposed a set of standard buffer solutions. Their pH values have been established from the emf of cells without a liquid junction. The operational definition of pH accepts the pH of these buffer solutions as correct [77].

For the pH range of 2 to 12 and for low ionic strength solutions ($<0.1 \text{ mol dm}^{-3}$), the measured pH using the method discussed should be within 0.02 of the correct value. Outside these ranges, errors in excess of 0.1 are possible.

C. Testing to Insure Suitability for Geochemical Metrology

To insure the applicability of SIROF pH electrodes for geochemical fluids, the SIROF electrodes will be evaluated for the environmental conditions of the particular repository site of interest. The environments of different repository sites may differ significantly in expected moisture, pH values, redox conditions, etc.

The proposed Tuff Repository in Yucca Mountain, Nevada has many features that make it attractive as a site for burial of nuclear waste material. The

repository is located approximately 400 meters below the surface in a compacted, hardened volcanic ash referred to as welded tuff. This level is about 100 meters above the water table. Water influx in the welded tuff is estimated to be less than one millimeter per year and the total moisture content is six percent by weight. Chemical analysis of groundwater [1] taken from Well J-13 indicates that the pH is near neutral at 7.1 and the concentrations for all ions is low. These ions are HCO_3 (120 ppm), SiO_2 (61 ppm), Na (51 ppm), SO_4 (22 ppm), Ca (14 ppm), Cl (7.5 ppm), NO_3 (5.6 ppm), K (4.9 ppm), F (2.2 ppm), and Hg (2.1 ppm). The water also contains 5 to 6 ppm of oxygen. The estimated temperature of a spent-fuel waste-package for a Tuff Repository [1] is less than 60°C during the operations period. However, it is estimated to be in the range 100 to 300°C during the thermal period of the first 300 years.

The nuclear waste will affect the long-term temperatures and pressures of the containment system. The pH sensors, therefore, must be able to withstand these elevated thermal conditions without undergoing changes in sensor properties.

The measurements of long-term stability and ionic interference at elevated temperatures have not been addressed before for SIROF electrodes. Laboratory simulation will be performed for these measurements up to 250°C and 600 psi in accordance with the environmental conditions for a Tuff Repository. The stability testing will be performed up to 30 days at various temperatures and pH levels. The selectivity of SIROFs will be investigated by studying the effect of various ionic species as previously described, on the electrode

response. Special attention will be paid to the ions of HCO_3 , SiO_2 , Na, SO_4 , and Ca, because these ions have higher concentration than other type of ions in the solutions in a Tuff Repository [1].

V. Summary

The pH values and ionic contents of geochemical solutions are important characteristics of a nuclear waste repository site [1]. The changes in solution chemistry conditions with time, which are likely to exist during the period of repository closure, must be taken into account if adequate containment is necessary for a long period. Therefore, the pH determination of the geochemical solution must be measured for long-term elevated thermal conditions.

Various metal oxide electrode materials have been described in a recent report and their application for measuring pH has been reviewed [2]. The requirements of a pH electrode for geothermal fluids are rather difficult to fulfil, e.g., the oxide must be stable at temperatures up to 250°C corrosion resistance, and robust, and exhibit a low sensitivity to ionic and redox interferences. Electrode materials of this type are discussed in the NBS/NRC review, of which the IrO_2 emerges as the most promising candidate because of its consistent near Nernstian response and its property of low impedance in thin films.

In order to optimize the performance of IrO_2 electrodes for pH sensing at

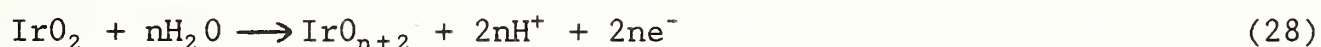
high temperatures and pressures, improved understanding of the electrochemical behavior at the IrO_2 -solution interface is essential. Electrochemical phenomena associated with the electrical charge and potential distribution in the interface have not been studied for SIROF-solution systems. The quantitative information can contribute to a better understanding of the electrode response, e.g., open circuit potential, stability, sensitivity, and selectivity.

For inorganic oxides, experimental studies have revealed the important role of H^+ and OH^- ions in determining the surface charge and potential. The classical GCSG model has been used by most colloid chemists in qualitatively interpreting observed phenomena at the oxide-liquid interface. Several workers have attempted to quantitatively describe the charge and potential distribution at the oxide-liquid interface using this model. Non-classical models have been proposed to account for the high surface charges observed for oxides. The porous double layer or gel layer model has been postulated in which H^+ and OH^- and counter ions are thought to penetrate into the solid oxide. However, independent measurements of oxide surface permeability cannot support porosity as a general model. The site-binding model involving surface complexation of protons and counter ions does appear to account for most observed experimental results.

Progress is obviously being made in the area of oxide-liquid interfaces. The basic phenomena are better understood, but it appears that no totally satisfactory model for the oxide-solution interface has emerged to date. Hydration, hydroxylation, and acid-base properties are all factors which

require special attention. As far as the iridium oxide-solution interface is concerned, two fundamental properties affecting the electrochemical behavior of hydrous iridium oxide films are (i) the acidity of the hydrated film and the variation of this property with change in the iridium oxidation state [57], and (ii) the difference in electrical conductivity between the reduced and oxidized form of the surface film [58,59]. According to Burke et al. [78,79] both properties are strongly influenced by the hydrated nature of the iridium oxide layer.

This report provides the general background and also some specific information regarding a number of oxide-liquid systems. However, this does not imply that the results from colloidal metal oxide studies can all be applied to the oxides used as pH electrodes. This is simply due to the lack of information presently available on the electrochemistry of the latter group of materials. Iridium oxide has a metal-like conductivity, so that there is no potential drop in the oxide. Its Fermi level is taken as the equilibrium potential of the electrode:



For these types of oxides having a metal-like conductivity the band structures are different from those of insulating oxides (band gaps greater than 3 eV) and of n-type or p-type semiconductors. Recently, theories for the metal-liquid and semiconductor-liquid systems have begun to appear, as well as models that attempt to model the interfaces realistically [80].

No attempt has been made so far to examine the GCSG theory's applicability to the IrO_2 -solution system. Interfacial phenomena for this

system are presently poorly understood. A detailed study of the capacitance properties of IrO_2 in contact with electrolyte pH solutions might give extremely valuable information concerning the dielectric properties of the contacting phases. The IrO_2 -solution system may be characterized by its capacitance-potential, capacitance-pH, capacitance-charge, and capacitance-time curves within the framework of the GCSG theory. This is of importance for interpretation of adsorption phenomena for H^+ , OH^- or other ions, of double layer effects in electrode reaction kinetics and of electrode instability in pH measurements. It is proposed that these capacitance characteristics may be obtained using d.c. and a.c. voltammetry.

REFERENCES

1. C. Interrante, E. Escalante, A. Fraker, M. Kaufman, W. Liggett, and R. Shull in Evaluation and Compilation of DoE Waste Package Test Data, NUREG/CR-4735, vol. 1 and 2 (1987).
2. T. Dietz and K. G. Kreider in Review of Materials for pH Sensing for Nuclear Waste Containment, NBS Interagency Report, No. 85-3237 (1985).
3. F. N. Hodges and L. R. Pederson, Materials Research Society, Abstracts of Fall Meeting (1987) 421.
4. M. J. Danielson, Corrosion, 35 (1979) 200: 39 (1983) 202.
5. L. W. Niedrach and W. H. Stoddard, J. Electrochem Soc., 131 (1984) 1017.
6. T. Tsuruta and D. D. Macdonald, J. Electrochem. Soc., 129 (1982) 1221.
7. T. Katsube, I. Lauks, and J. N. Zemel, Sensors and Actuators, 2 (1982) 399.
8. J. Lyklema, Croat. Chem. Acta 43 (1971) 249.
9. J. Lyklema in Th.F. Tadros (Ed), Solid/Liquid Dispersions, Academic Press, New York (1987) Ch. 3.
10. S. M. Ahmed in J. W. Diggle (Ed.), Oxides and Oxide Films, Vol. 1, Marcel Dekker, New York (1972) Ch. 4.
11. R. J. Hunter, Foundations of Colloid Science, Vol. 1, Clarendon Press, Oxford (1987) Ch. 6.
12. R. Parsons in A. F. Silva (Ed.), Trends in Interfacial Electrochemistry, D. Reidel Publishing Co., Boston (1986) 373.
13. R. Parsons in J. O'M. Bockris and B. E. Conway (Eds.), Modern Aspects of Electrochem, Vol. 1, Butterworths, London (1954) 103.
14. S. Levine, J. Mingins and G. M. Bell, J. Electroanal. Chem. 13 (1967)

280.

15. S. Levine, G. M. Bell and D. Calvert, *Can. J. Chem.* 40 (1962) 518.
16. L. Blok and P. L. de Bruyn, *J. Colloid Interface Sci.* 32 (1970) 518, 527, 533.
17. S. M. Ahmed and D. Maksimov, *J. Colloid Interface Sci.* 29 (1969) 97.
18. Th. F. Tadros and J. Lyklema, *J. Electroanal. Chem.* 17 (1968) 267.
19. H. C. Li and P. L. de Bruyn, *Surf. Sci.* 5(1966) 203.
20. G. H. Bolt, *J. Phys. Chem.* 61 (1957) 1166.
21. A. Breeuwsma and J. Lyklema, *dis. Faraday Soc.* 52 (1971) 324.
22. D. E. Yates and T. W. Healy, *J. Colloid Interface. Sci.* 52 (1975) 222.
23. Y. G. Berube and P. L. de Bruyn, *J. Colloid Interface Sci.* 28 (1968) 92.
24. E. Herszynska, *J. Inorg. Nucl. Chem.*, 26 (1964) 2127.
25. C. P. Huang and W. Stumm, *J. Colloid Interface Sci.* 43 (1973) 409.
26. J. J. Morgan and W. Stumm, *J. Colloid Interface Sci.* 19 (1964) 347.
27. J. Lyklema, *J. Electroanal. Chem.* 18 (1968) 341.
28. Th. F. Tadros and J. Lykema, *J. Electroanal. Chem.* 17 (1968) 267.
29. Th. F. Tadros and J. Lyklema, *J. Electroanal. Chem.* 22 (1969) 1.
30. J. W. Perram, *J. Chem. Soc. Faraday II* 2 (1973) 993.
31. J. W. Perram, R. J. Hunter, and H. J. L. Wright, *Chem. Phys. Lett.* 23 (1973) 265.
32. J. W. Perram, R. J. Hunter, and H. J. L. Wright, *Aust. J. Chem.* 27 (1974) 461.
33. M. J. Dignam, *Can. J. Chem.* 56 (1978) 595.
34. M. J. Dignam and R. K. Kalia, *Surf. Sci.* 100 (1980) 154.
35. T. W. Healy and L. R. White, *Adv. Colloid Interface Sci.* 9 (1978) 303.

36. D. E. Yates, S. Levine, and T. W. Healy, *J. Chem. Soc. Faraday I* 70 (1974) 1807.
37. J. A. Davis, A. P. James, and J. O. Leckie, *J. Colloid Interface Sci.* 63 (1978) 480.
38. R. O. James and G. A. Parks, *Surf. Colloid Sci.* 12 (1982) 119.
39. G. W. Wang, D. Yu and Y. L. Wang, *Sensors and Actuators*, 11 (1987) 221.
40. D. L. Harnage, L. J. Bousse, J. D. Shott and J. D. Meindl, *IEEE Trans. Electron Devices*. ED-34 (1987) 1700.
41. A. Van Den Berg, P. Bergveld, D. N. Reinhoudt and E. J. R. Sudholter, *Sensors and Actuators*, 8 (1985) 129.
42. L. D. Burke and M. E. G. Lyons in *Modern Aspects of Electrochemistry*, R. E. White, J. O'M. Bockris and B. E. Conway (Eds.), Plenum press, New York 18 (1986) Ch. 4.
43. D.N. Buckley and L.D. Burke, *J. Chem. Soc. Faraday Trans.* 171 (1975) 1447.
44. D.A.J. Rand and R. Woods, *J. Electroanal. Chem.* 55 (1974) 375.
45. L.D. Burke and M.B.C. Roche, *J. Electroanal. Chem.* 164 (1984) 315.
46. G. Belanger and A.K. Vijh, in *Oxide and Oxide Films*, vol. 5, Ed. by A.K. Vijh, Marcel Dekker, New York, 1977, pp. 1-104.
47. J. Mozota and B.E. Conway, *Electrochim. Acta.* 28 (1983) 1.
48. D.N. Buckley, L.D. Burke, and J.K. Mulcahy, *J. Chem. Soc. Faraday Trans. I.*, 72 (1976) 1896.
49. B.E. Conway and J. Mozota, *Electrochim. Acta* 28 (1983) 9.
50. L.D. Burke, J.K. Mulcahy, and D.P. Whelan, *J. Electroanal. Chem.* 163 (1984) 117.

51. M.S. Cruz, T.F. Otero, and S.U. Zanartu, J. Electroanal. Chem. 158 (1983) 375.
52. D. Mitchell, D.A.J. Rand, and R. Woods, J. Electroanal. Chem. 84 (1977) 117.
53. S.Gottesfeld and S. Srinivasan, J. Electroanal. Chem. 86 (1978) 89.
54. J.D.E. McIntyre, W.F. Peck, and S. Nakahara, J. Electrochem. Soc. 127 (1980) 1264.
55. S. Hackwood, A.H. Dahem, and G. Beni, Phys., Rev. B26 (1982) 471.
56. J. Augustynski, M. Kondelka, J. Sanchez, and B.E. Conway, J. Electroanal. Chem. 160 (1984) 233.
57. L.D. Burke and D.P. Whelan, J. Electroanal. Chem. 162 (1984) 121.
58. S.H. Glarum and J.H. Marshall, J. Electrochem. Soc. 127 (1980) 1467.
59. S. Gottesfeld, J. Electrochem. Soc. 127 (1980) 1922.
60. L. D. Burke and D.P. Whelan, J. Electroanal. Chem 124 (1981) 333.
61. J. D. E. McIntyre, S. Basu, W. F. Peck, W. L. Brown, and M. W. Augustyniak, Phys. Rev. B25 (1982) 7542.
62. J.D.E. McIntyre, S. Basu, W.F. Peck, W.L. Browne, and W.M.Augustyniak, Solid State Ionics 5 (1981) 359.
63. J.D.E. McIntyre, J. Electrochem. Soc. 126 (1979) 2171.
64. G. Beni, C.E. Rice, and J.L. Shay, J. Electrochem. Soc. 127 (1980) 1342.
65. G. Beni and J.L. Shay, Appl. Phys. Lett., 33 (1978) 567.
66. S. Hackwood, G. Beni W.C. Dautremont-Smith, L.M. Shiavone, and J.L. Shay, Appl. Phys. Lett. 37 (1980) 965.
67. C.E. Rice, Appl. Phys. Lett. 35 (1979) 563.
68. S. Gottesfeld, J. Electrochem. Soc. 127 (1980) 1922.
69. J.O. Zerbino and A.J. Arvia, J. Electrochem. Soc. 126 (1979) 93.

70. L.D. Burke and R.A. Scannell, J. Electroanal. Chem. 175 (1984) 119.
71. M. F. Yuen and I. Lauks, Solid State Ionics, II (1983) 19.
72. A. Fog and R. P. Buck, Sensors and Actuators, 5 (1984) 137.
73. K. Kinoshita and M. J. Maden, J. Electrochem. Soc. 131 (1984) 1089.
74. K. G. Kreider, S. Semanick, J. W. Erickson, Proc. 4th Internl. Conf. Sensors and Actuators (Transducers '87), Tokyo, Japan (1987) 734.
75. S. M. Faynor in Laboratory Instrumentation (3rd Ed.), J. B. Kppincott Co., Philadelphia (1987) Ch. 9.
76. H. L. Trietley in Transducers in Mechanical and Electronic Design, Marcel Dekker, Inc., New York (1986) Ch. 6.
77. Y. C. Wu, W. F. Koch, and G. Marinenko, J. Research, NBS 89 (1984) 395.
78. L. D. Burke and D. P. Whelan, J. Electroanal. Chem. 124 (1981) 333.
79. L. D. Burke, M. E. Lyons, E. J. M. O'Sullivan, and D. P. Whelan, J. Electroanal. Chem. 122 (1981) 403.
80. J. Goodisman, Electrochemistry: Theoretical Foundations, John Wiley & Sons, New York (1987) Ch. 5.

U.S. DEPT. OF COMM. BIBLIOGRAPHIC DATA SHEET (See instructions)	1. PUBLICATION OR REPORT NO. NBSIR 88-3790	2. Performing Organ. Report No.	3. Publication Date MAY 1988
4. TITLE AND SUBTITLE Electrochemical Evaluation of Solid State pH Sensors for Nuclear Waste Containment			
5. AUTHOR(S) Peter H. Huang and Kenneth G. Kreider			
6. PERFORMING ORGANIZATION (If joint or other than NBS, see instructions) NATIONAL BUREAU OF STANDARDS DEPARTMENT OF COMMERCE WASHINGTON, D.C. 20234		7. Contract/Grant No.	8. Type of Report & Period Covered
9. SPONSORING ORGANIZATION NAME AND COMPLETE ADDRESS (Street, City, State, ZIP) Nuclear Regulatory Commission Office of Research Washington, DC 20555			
10. SUPPLEMENTARY NOTES <input type="checkbox"/> Document describes a computer program; SF-185, FIPS Software Summary, is attached.			
11. ABSTRACT (A 200-word or less factual summary of most significant information. If document includes a significant bibliography or literature survey, mention it here) This report contains a literature review for electrochemical evaluation of solid state pH sensors. The requirements of pH electrode for geochemical fluids in a nuclear waste repository site are rather difficult to fulfill, that is, the electrode must have stability at temperatures up to 250°C, low ionic and redox interferences, corrosion resistance, and robustness. Among the potential electrode materials, the IrO ₂ emerges as the most promising because of its consistent near Nernstian response and its property of low impedance in thin films. However, improved understanding of the electrochemical behavior at the IrO ₂ -solution interface is essential in order to optimize the performance of IrO ₂ electrodes for pH sensing at high temperatures and pressures. This report reviews theoretical models of the oxide-solution interfaces based on the theory of the electric double layer. Electrochemistry of IrO ₂ films with emphasis on the properties of anodic films is summarized. A plan for pH testing of sputtered iridium oxide films (SIROF) for geochemical measurements at a Tuff Repository is described.			
12. KEY WORDS (Six to twelve entries; alphabetical order; capitalize only proper names; and separate key words by semicolons) electric double layer; electrochemistry; iridium oxide; oxide-solution interface; pH sensors; votammetry			
13. AVAILABILITY <input checked="" type="checkbox"/> Unlimited <input type="checkbox"/> For Official Distribution. Do Not Release to NTIS <input type="checkbox"/> Order From Superintendent of Documents, U.S. Government Printing Office, Washington, D.C. 20402. <input checked="" type="checkbox"/> Order From National Technical Information Service (NTIS), Springfield, VA. 22161		14. NO. OF PRINTED PAGES 35	15. Price \$11.95

